What controls CCN seasonality in the Southern Ocean? A statistical analysis based on satellite-derived chlorophyll and CCN and model-estimated OH radical and rainfall

S. M. Vallina,[1] R. Simó,[1] and S. Gassó[2]

Received 29 July 2005; revised 3 November 2005; accepted 17 November 2005; published 8 March 2006.

[1] A 3-year time series set (from January 2002 to December 2004) of monthly means of satellite-derived chlorophyll (CHL) and cloud condensation nuclei (CCN), as well as model outputs of hydroxyl radical (OH), rainfall amount (RAIN), and wind speed (WIND) for the Southern Ocean (SO, 40°S–60°S) is analyzed in order to explain CCN seasonality. Chlorophyll is used as a proxy for oceanic dimethylsulfide (DMS) emissions since both climatological aqueous DMS and atmospheric methanesulfonate (MSA) concentrations are tightly coupled with chlorophyll seasonality over the Southern Ocean. OH is included as the main atmospheric oxidant of DMS to produce CCN, and rainfall amount as the main loss factor for CCN through aerosol scavenging. Wind speed is used as a proxy for sea salt (SS) particles production. The CCN concentration seasonality is characterized by a clear pattern of higher values during austral summer and lower values during austral winter. Linear and multiple regression analyses reveal high significant correlations between CCN and the product of chlorophyll and OH (in phase) and rainfall amount (in antiphase). Also, CCN concentrations are anticorrelated with wind speed, which shows very little variability and a slight wintertime increase, in agreement with the sea salt seasonality reported in the literature. Finally, the fraction of the total aerosol optical depth contributed by small particles (ETA) exhibits a seasonality with a 3.5-fold increase from austral winter to austral summer. The biogenic contribution to CCN is estimated to vary between 35% (winter) and 80% (summer). Sea salt particles, although contributing an important fraction of the CCN burden, do not play a role in controlling CCN seasonality over the SO. These findings support the central role of biogenic DMS emissions in controlling not only the number but also the variability of CCN over the remote ocean.

Citation: Vallina, S. M., R. Simó, and S. Gassó (2006), What controls CCN seasonality in the Southern Ocean? A statistical analysis based on satellite-derived chlorophyll and CCN and model-estimated OH radical and rainfall, *Global Biogeochem. Cycles*, *20*, GB1014, doi:10.1029/2005GB002597.

1. Introduction

[2] Since *Charlson et al.* [1987] suggested that marine algae participate in climate regulation through the production of the cloud precursor dimethylsulfide (the CLAW hypothesis,so called after the authors' initials), much experimental effort has been invested into seeking for links between oceanic plankton and tropospheric aerosols. Many marine phytoplankton taxa produce intracellular dimethylsufoniopropionate (DMSP), the biochemical precursor of dimethylsulfide (DMS), with important physiological functions [*Stefels*, 2000; *Sunda et al.*, 2002]. DMSP is partly converted to DMS by enzymatic cleavage with involvement of the whole planktonic food web [*Simó*, 2001].

[3] In seawater, DMS undergoes bacterial consumption and photolysis, and a fraction of it is ventilated from the oceans to the atmosphere following Henry's law. The ventilation rate depends not only on aqueous DMS concentration (DMSw) but also on seawater temperature and wind speed [*Liss and Merlivat*, 1986]. Once in the atmosphere DMS (DMSa) undergoes a sequence of oxidative reactions through interaction mainly with the hydroxyl radical (OH), giving rise to a range of products. Among them, non-sea-salt sulfate (nss-SO_4) and, to a lesser extent, methanesulfonate (MSA) are of particular interest because of their potential role to form cloud condensation nuclei (CCN) [*Cox*, 1997]. MSA and SO_4 particles are highly hygroscopic and mainly occur in the submicron size fraction, ranging between 0.1 and 1 μm in diameter, which is also the optimal

[1] Institut de Ciències del Mar–Consejo Superior de Investigaciones Científicas (ICM–CSIC), Barcelona, Spain.
[2] Goddard Earth Science and Technology Center, University of Maryland Baltimore County, Baltimore, Maryland, USA.

0886-6236/06/2005GB002597$12.00

size range for CCN [*Ayers et al.*, 1997, 1999; *Andreae et al.*, 1999; *Jourdain and Legrand*, 2001].

[4] DMS emission is, by far, the largest natural source of volatile sulfur to the atmosphere [*Andreae and Crutzen*, 1997; *Simó*, 2001]. Global emissions are estimated in the range of 16 to 24 TgS yr^{-1} [*Kettle and Andreae*, 2000; *Chapman et al.*, 2002]. Even though this represents between 25 and 35% of the estimated anthropogenic sulfur emissions (65 TgS yr^{-1}) [*Benkovitz et al.*, 1996] DMS accounts for essentially all nss-SO_4 in vast regions of the remote oceans [*Savoie and Prospero*, 1989]. The Southern Ocean (SO) atmosphere is regarded as one of the most unpolluted over the world [*Buseck and Pósfai*, 1999], where the aerosol is expected to be minimally perturbed by either anthropogenic or natural continental sources [*Quinn et al.*, 1998; *Andreae et al.*, 1999; *Ayers and Gillett*, 2000; *Gabric et al.*, 2001; *Prospero et al.*, 2002]. The SO is, therefore, the most appropriate region for testing the validity of the CLAW hypothesis, or at least some of their central statements.

[5] Several short- and long-term observational studies carried out at sites in the SO, from temperate to Antarctic regions, have shown a strong coupling between DMS, its atmospheric oxidation products, and CCN [e.g., *Prospero et al.*, 1991; *Ayers and Gras*, 1991; *Ayers et al.*, 1997; *Andreae et al.*, 1999; *Jourdain and Legrand*, 2001]. By reviewing the large body of data collected at Cape Grim, *Ayers and Gillett* [2000] confirmed the strong seasonal coupling between DMSa, MSA and nss-SO_4, and also reported direct evidence for the coupling between DMS, CCN and cloud droplet numbers. Also, during the First Aerosol Characterization Experiment (ACE 1), *Brechtel et al.* [1998] found that an increase in the number of particles in the Aitken and accumulation modes was associated with an air mass transported over warm DMS-rich waters. These findings strongly suggest a central role of oceanic DMS as a precursor of CCN in the SO, at least during the biologically productive season.

[6] Because of the obvious geographic sparseness of atmospheric sampling stations, there is a lack of studies on regional or global scales. Optical sensors on satellites (e.g., NASA's SeaWiFS and MODIS) offer the possibility of making quasi-synoptic, reliable and with high spatial resolution simultaneous measurements of ocean and atmospheric variables at large scales. With such new methodology and data, it is possible to investigate if the connection between marine microbiota, aerosols and clouds found in local studies also holds at the larger spatial and temporal scales that are relevant for potential climate regulation.

[7] A pioneering work on the use of satellite data for testing plankton-aerosol links has been done by *Gabric et al.* [2002] for a region of the SO south of Australia (from 40°S to 53°S and from 126°E to 148°E). They found evidence for a coupling between CHL and total aerosol optical depth (AOD) at multiple scales, from weekly to seasonal. However, they could not resolve whether this coupling was mainly due to aerosol fertilization of productivity or biogenic effects on aerosol production. Here we present a continuation of the work of *Gabric et al.* [2002] by going further in several aspects: (1) We focus on the whole Southern Ocean (40°S–60°S). (2) We use a new generation of algorithms for the derivation of CCN concentrations from the primary aerosol products of MODIS. (3) Two other variables are taken into account as a priori important factors controlling the seasonality of CCN: the OH radical concentration in the marine boundary layer and the rainfall amount; simple and multiple linear statistical models are applied in order to test the effect of the inclusion of OH and rainfall estimates on the observed variance of CCN numbers. (4) The seasonality of the fine mode aerosols is also discussed.

2. Characteristics of the Study Region: Productivity, DMS, and Wind

[8] The study region covers the whole SO, defined as the area comprised between 40°S and 60°S (see Figure 1). The latitudinal range covers roughly two major water bodies: the Sub-Antarctic Zone (SAZ) (40°S–53°S) and the Antarctic Zone (AZ) (53°S–60°S) [*Curran and Jones*, 2000]. We purposely exclude from our study the potential effects of the sea-ice formation and melt; with this aim, we omit latitudes south of 60°S (the Seasonal Ice Zone or SIZ), a general limit for maximum Antarctic sea-ice coverage [*Prospero et al.*, 1991; *Rasmus et al.*, 2004]. The northern part of the region is flanked by the Subtropical Front (about 40°S), which is considered the upper limit of the SO [*Boyd*, 2002]. In the southern part the Antarctic Polar Front (APF) is present (between 45°S and 60°S) and characterized by upwelling eddies and higher phytoplankton biomass in its southernmost edge [*Moore et al.*, 1999].

[9] Over the year, most of the SO exhibits moderate CHL concentrations, generally less than 0.3–0.4 mg m^{-3}. Phytoplankton blooms that give rise to CHL concentrations higher than 1 mg m^{-3} are present in shelf waters, the vicinity of major fronts, and sea-ice retreat zones [*Moore and Abbott*, 2000]. CHL peaks during the summer and is depressed in winter [*Curran and Jones*, 2000; *Gabric et al.*, 2002]. This seasonality is believed to be driven by the depth of the mixed layer (ML) [*Rasmus et al.*, 2004], which varies from maxima around 400 m in winter to less than 30 m in summer [*de Boyer-Montégut et al.*, 2004]. In all seasons but summer, the deep mixed layer depth (MLD) imposes a severe light limitation to phytoplankton growth (probably light-iron colimitation) [*Boyd*, 2002] even though macronutrient concentrations are amongst the highest of the world's oceans. During summer, phytoplankton is only limited by iron [*Boyd*, 2002].

[10] There is compelling observational evidence that the seasonality of DMSP and DMSw concentrations, as well as DMS emission fluxes, follows the seasonality of phytoplankton in the SO [*Turner and Owens*, 1995; *Gabric et al.*, 1996; *Ayers et al.*, 1995, 1997; *Kettle et al.*, 1999; *Curran and Jones*, 2000; *Ayers and Gillett*, 2000; *Simó and Dachs*, 2002]. This is a distinct feature of the SO with respect to subtropical regions and temperate regions of the Northern Hemisphere, where maximum surface DMS concentrations occur associated with low CHL levels in highly irradiated, shallow stratified waters during summer

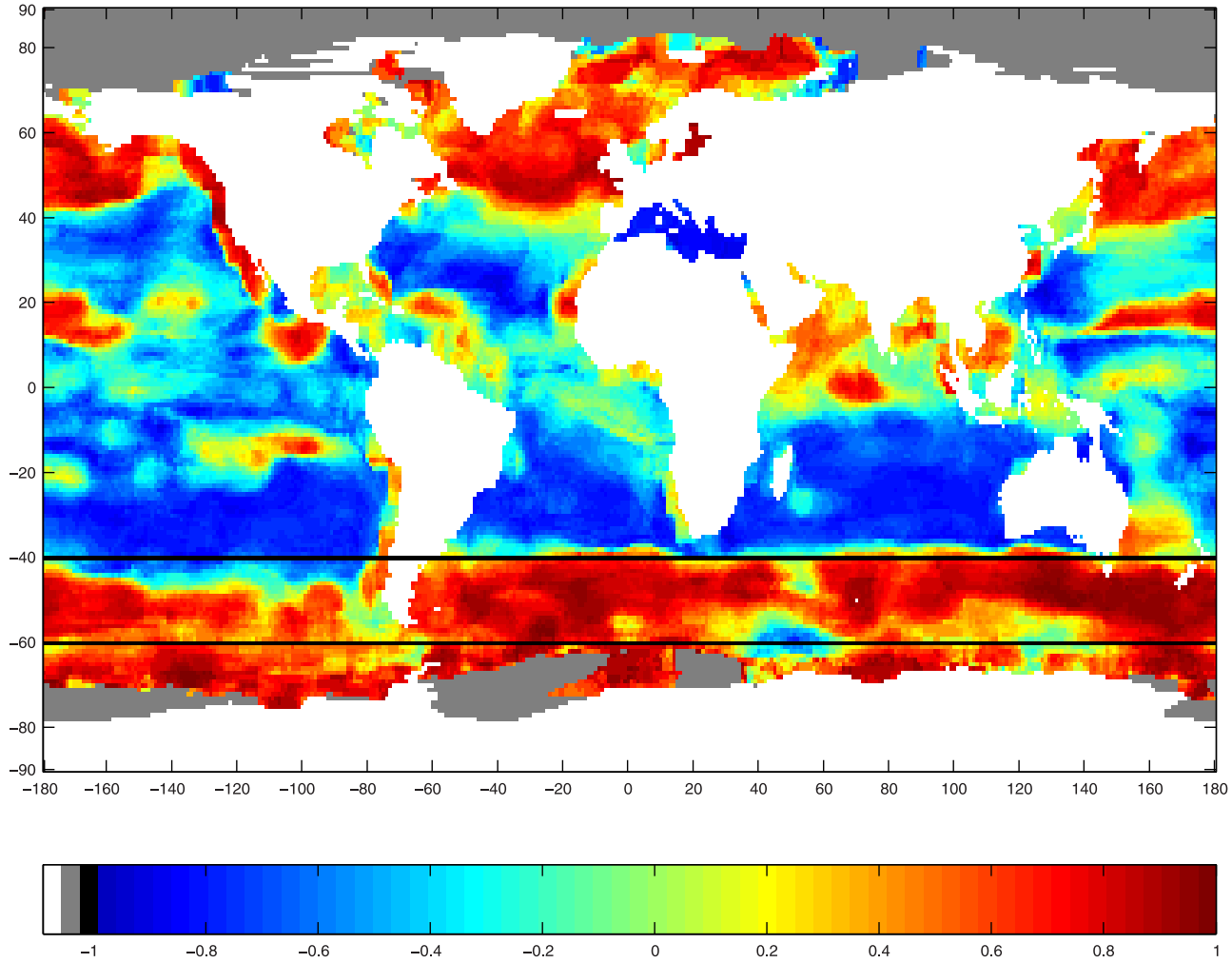

Figure 1. Global map of seasonal correlations between climatological monthly aqueous DMS concentrations (from *Kettle and Andreae* [2000]) and climatological monthly CHL concentrations (from SeaWiFS, means of years 2002 to 2004). The Southern Ocean study region is the area between the two black lines.

[*Dacey et al.*, 1998; *Simó and Pedrós-Alió*, 1999; *Simó and Dachs*, 2002; *Toole and Siegel*, 2004]. Globally mapped, $7^\circ \times 7^\circ$ running window correlations between monthly CHL (SeaWiFS, average of 2002–2004) and DMSw [*Kettle and Andreae*, 2000] climatologies show strong positive and almost homogeneously distributed correlations over the SO region (Figure 1; significant correlations for $|r| > 0.5$). However, it is important to point out that the DMSw climatology is based on a compilation of DMSw measurements and they make use of an interpolation procedure to fill the large areas/seasons where no data are available. Annual time series of atmospheric DMS and MSA concentrations at Cape Grim also exhibit a pattern very similar to that of oceanic DMS and CHL [*Ayers and Gillett*, 2000]. The Spearman correlation coefficient between monthly CHL (averaged for the SO over the period 2002–2004) and monthly MSA at Cape Grim (averaged over the period 1988–1996) is very high ($\rho = 0.97$; $p - val \ll 0.001$). Since DMS cannot be remotely sensed from satellite, and in the absence of gridded, spatially comprehensive data on DMSw simultaneous to that of CCN, we use satellite-derived CHL data, which offer such a coverage, as a proxy for DMSw. We, hereby, presume that any trends CHL might show in our analyses will be representative of those of DMSw.

[11] The SO experiences the highest wind speeds of the globe with a persistent wind field and rich storm activity [*Yuan*, 2004]. Winds flow eastward most of the time for most of the region (the "roaring forties"), with the meridional component (mainly southward) being much weaker than the zonal component [*Gille*, 2005]. Interestingly, the wind stress at 55°S shows little seasonal variability in contrast to other regions of the globe [*Gille*, 2005]. On a regional average, wind speed seasonal amplitude is less than ±10% of the annual mean (10.5 m s^{-1}; see Figure 2h). In consequence, the variability of the DMS emission flux (the

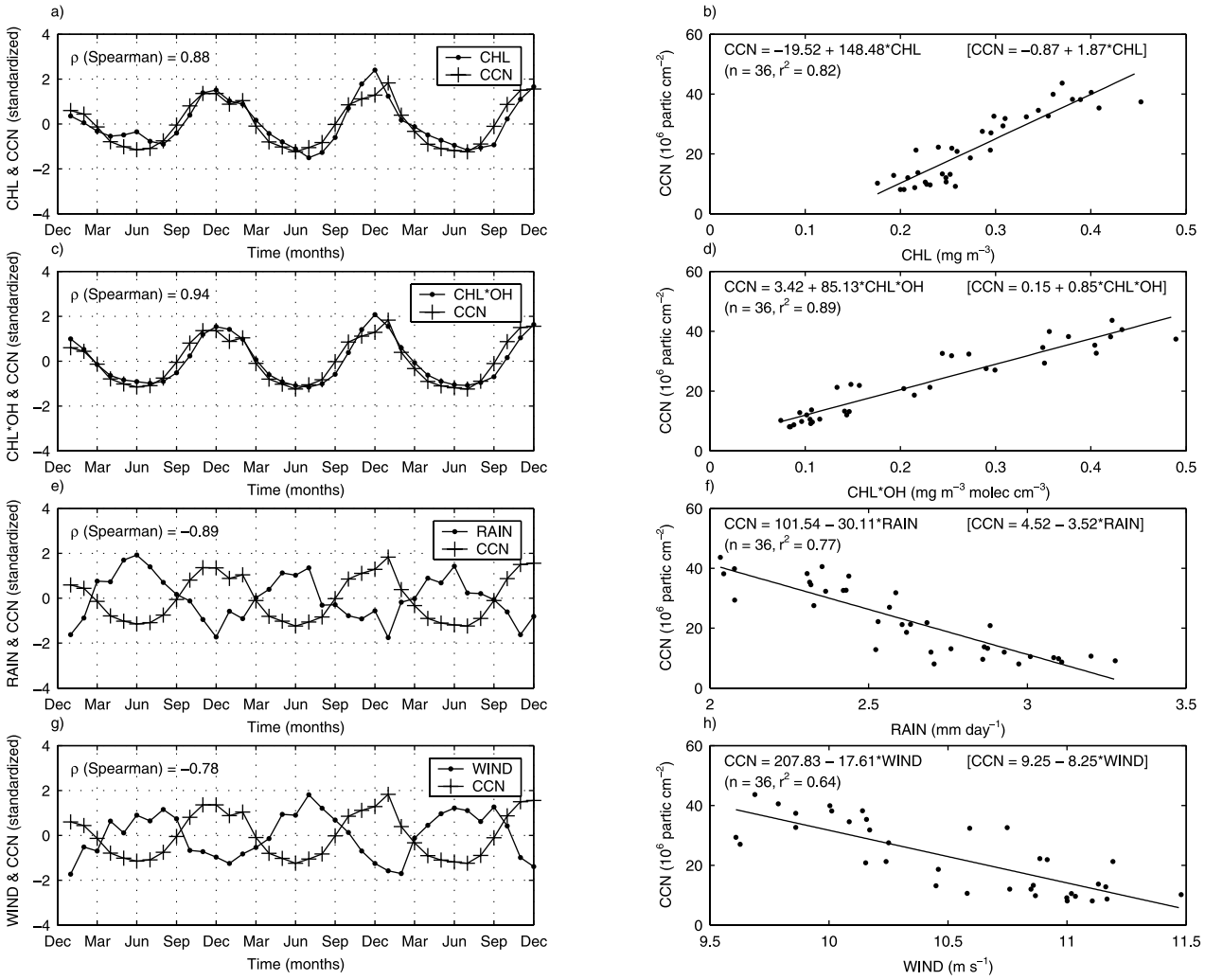

Figure 2. Seasonal evolution (years 2002 to 2004) and the associated Spearman correlation coefficient of CCN against (a) chlorophyll, (c) chlorophyll*hydroxyl radical, (e) rainfall amount, and (g) wind speed (variables are presented in standardized form, i.e., subtracting the mean and dividing by the standard deviation). Regression analyses of CCN against (b) chlorophyll, (d) chlorophyll*hydroxyl radical, (f) rainfall amount, and (h) wind speed. CCN values are derived from MODIS according to *Gassó and Hegg* [2003]. Chlorophyll concentrations are obtained from SeaWiFS. Hydroxyl radical concentrations are outputs of the GEOS-CHEM model provided by the Atmospheric Chemistry Modeling Group at Harvard University [*Fiore et al.*, 2003]. Rainfall amount and wind speeds are obtained from the NCEP/NCAR Reanalysis Project. Note the little seasonal variability of the wind speed (less than ±10% of the annual mean). Equations in brackets represent the linear regressions applied to normalized data sets by dividing the individual monthly values by the annual mean.

source of atmospheric DMS) is driven mainly by the variability of DMSw concentrations. That is, we are using CHL as a proxy for DMS emissions.

3. Data and Methodology

3.1. Data Sets: Sources and Justification

[12] The Sea-viewing Wide Field-of-view Sensor (SeaWiFS) flies on the OrbView-2 (formerly "SeaStar") platform and it measures radiances in eight spectral bands (from 0.40 to 0.88 μm). SeaWiFS estimates the ocean surface CHL concentration (mg m^{-3}) based on the ratio between reflectance in two visible channels (0.49 μm for blue and 0.55 μm for green) [*Yang and Gordon*, 1997]. Higher reflectance in the green channel corresponds to waters with higher CHL concentrations. The MODerate resolution Imaging Spectro-radiometer (MODIS), on board the Earth Observing System (EOS), currently has two detector in orbit (in the satellites Terra and Aqua). Both have daily global coverage with a morning and afternoon pass, respectively. In this study, we used data measured by MODIS-Terra. MODIS acquires data globally at 36 spectral bands

(from 0.4 to 14.5 μm). Several aerosol parameters are retrieved from MODIS daytime data over the ocean, including the fine mode fraction or ETA parameter [*Remer et al.*, 2005]. Ranging from 0 to 1, ETA is defined as the ratio of the AOD contributed by the small mode particles (or accumulation mode) to the total AOD (AOD_{small}/AOD_{total}) and can thus be viewed as a measure of the proportion of fine mode particles that contribute to the total aerosol extinction. In this study we use the ETA parameter to infer the seasonality of the dominant aerosol types in the SO. Coarse mode particles are mostly dominated by sea salt (SS) and dust, while nss-SO_4 and carbonaceous aerosols are more common in the accumulation mode. Because the lack of constant anthropogenic sources and minimal dust activity in the SO, SS and nss-SO_4 aerosols are the dominant aerosol types. Thus the seasonality of the ETA parameter allows us to infer the relative contribution of SS and nss-SO_4 particles for each season. We would like to note that MODIS also provide CHL estimates but it lacks the SeaWiFS capability to tilt away to avoid sunglint (the specular reflection of sunlight from the sea surface). Then SeaWiFS CHL retrievals are of higher accuracy. Either the SeaWiFS CHL data (9 km × 9 km resolution) and the MODIS aerosol data (1° × 1° resolution) used are available from NASA's Goddard Space Flight Center (GSFC) Distributed Active Archive Centers (DAAC).

[13] From the primary parameters retrieved by MODIS (AOD, ETA and Effective radius), it is possible to derive secondary products such as column-integrated CCN concentration (in units of partic cm^{-2}) [*Tanré et al.*, 1999; *Gassó and Hegg*, 2003]. In the present work, CCN concentrations are obtained with the derivation method described by *Gassó and Hegg* [2003]. The method derives the maximum number of particles in the accumulation mode and provides an upper end estimate of the concentration of particles that may act as CCN at ≈0.2% supersaturation. The method allows for the adjustment of coefficients according to the type of aerosols that are present. Since we are focusing on the SO, the CCN algorithm coefficients (the aerosol refraction index and the aerosol density) were adjusted to be representative of the main aerosol types present in this marine remote region: SS, nss-SO_4 and MSA.

[14] In order to compare the obtained column-integrated values (partic cm^{-2}) to in situ measurements of CCN concentrations (partic cm^{-3}) we assume that most of the CCN occur in the marine boundary layer (MBL) [*Gassó and Hegg*, 2003]. The height of the MBL is assumed to vary with the seasons (typically 600 m in winter and 1400 m in summer). We obtain averaged CCN concentrations of 157 partic cm^{-3} in winter and 266 partic cm^{-3} in summer, which are about a factor of 2.8 higher than Cape Grim measurements of CCN at 0.23% supersaturation (55 partic cm^{-3} in winter and 95 partic cm^{-3} in summer [*Ayers and Gras*, 1991]). In contrast, the seasonal variability is well captured: the summer-maximum to winter-minimum ratio is about 1.7 for both satellite-derived and in situ measured CCN concentrations. Similar overestimates are obtained using annual averages of CCN and an average MBL of 1000 m (225 partic cm^{-3} from MODIS against 75 partic cm^{-3} at Cape Grim). However, the general assumption that most of the CCN particles occur in the MBL does not seem to hold always over the SO. Summer vertical distributions of CCN obtained by *Hudson et al.* [1998] between 40°S–55°S and 135°E–160°E showed that CCN are present up to 400 mb (roughly about 7000 m). This could explain the high column-integrated values of CCN retrieved from the satellite and the apparent overestimation of the calculated concentrations based on an air column of only 1000 m. With an air column of 7000 m, satellite CCN concentrations would be ≈53 partic cm^{-3} in summer, which is lower than those measured at Cape Grim but within the range of those measured by *Hudson et al.* [1998] during the flights.

[15] Global and regional OH concentrations in the MBL are outputs of the GEOS-CHEM model run by the Atmospheric Chemistry Modeling Group at Harvard University [*Fiore et al.*, 2003]. GEOS-CHEM simulates atmospheric composition using assimilated meteorological observations from the Goddard Earth Observing System (GEOS) of the NASA Global Modeling and Assimilation Office. Including OH variability when seeking for a causal relationship between DMS and CCN seems necessary since OH is the main oxidizer of atmospheric DMS to produce CCN. Not taking in account its contribution would artificially increase the DMS weight in the statistical analysis of the CCN seasonality because OH experiences a strong reduction during the darker winter months. Surface wind speed (WIND) and rainfall amount (RAIN) were obtained from the NCEP/NCAR Reanalysis data provided by the NOAA-CIRES Climate Diagnostics Center. The NCEP/NCAR Reanalysis project uses a state-of-the-art analysis/forecast system to perform data assimilation using contemporary data. We used monthly maps of both variables at a 2.5° × 2.5° resolution. Both WIND (m s^{-1}) and RAIN (mm d^{-1}, also referred to as "precipitation rate" by NCEP) are model outputs. WIND is better constrained by contemporary data obtained from the SSM/I sensor (DMSP, NOAA). On the other hand, there are no real rainfall observations directly constraining the variable RAIN, so that it is derived solely from the model fields forced by the real atmospheric assimilated data [*Kistler et al.*, 2001].

[16] The variables CHL, CCN, ETA, WIND, and RAIN are level 3 monthly composites for the period between January 2002 and December 2004. The multiyear time series is meant to capture the interannual variability. Monthly OH distributions, however, were available only for 2001. We assume that the OH interannual variability is low and then we have repeated three times the modeled OH annual cycle to obtain 3 years. We then calculate the mean value of each variable for each month over the whole SO area covered (36 data points). With this averaging procedure, the spatial distribution of the variables is not taken into account, with the assumption that they are rather homogeneously distributed. This is certainly not true for CHL, but it is closer to reality for OH and CCN owing to the strong eastward wind conditions. Owing to the faster motion of air masses than oceanic currents (and not necessarily coincident directions), any potential effect of oceanic CHL on atmospheric CCN can only be observed at spatial scales much larger than local. The choice of the monthly time frame pursues to focus on the seasonal patterns and to reduce from

the statistical analysis the effect of potential time lags existing between aerosol-precursor (mainly DMS) production by the marine biota (CHL) and the formation of CCN by atmospheric oxidation of this precursor.

[17] Since the development of a phytoplankton bloom to the rise of aqueous DMS concentrations the time lag can range from hours to days, mainly driven by algal physiological stress, cell mortality, viral activity and zooplankton grazing. During the SOIREE mission, for instance, an increase in primary production was induced by adding iron to the surface waters [*Boyd et al.*, 2000]. A significant increase in DMS concentrations was observed 5 days after the rise in *Prymnesiophyte* abundances and 2 days after the bulk CHL rise, coinciding with the response of zooplankton grazers. There is strong evidence for direct DMS exudation from phytoplankton when cells are under stressing conditions of high UV exposure and iron limitation [*Sunda et al.*, 2002] such as those encountered in the surface SO during summer. In this case there would not exist a lag between CHL and DMS. On top of that, we should add the time needed for DMS to be ventilated to the atmosphere, oxidized to SO_2 and subsequently to nss-SO_4 (gas-to-particle conversion) [*Fitzgerald*, 1991]. Ventilation is rapid owing to the high wind speeds, and the summer DMSa lifetime in our study region is estimated to be 12–24 hours [*Bates et al.*, 1998; *Mari et al.*, 1998] although in winter it is in the order of a week [*Gabric et al.*, 1996]. Lifetime of SO_2 is normally less than 1 day [*Shon et al.*, 2001].

[18] Taking it all together, we estimate that any time lag between CHL and CCN concentrations through DMS should be seasonally variable but in the range of few days in summer to 2 weeks in winter at the most. Therefore, using a time resolution of 1 month (monthly means) we should be able to capture most of the CHL–CCN cycle, at least in the productive season. To explore the importance of a potential lag between CHL and CCN, we repeat the statistical analysis after applying a lag of half a month to (only) the atmospheric variables: $y^* = (y_i + y_{i+1})/2$ (where $i = 1, .., 36$ are months, y_i is the value of either OH, CCN or RAIN for the month i, and y^* is the lagged value).

[19] Rainfall acts as an aerosol scavenger either by in-cloud scavenging as well as by below-cloud washout. Therefore the two main loss factors influencing CCN concentrations are the nucleation process, which changes the status of a particle from CCN to cloud droplet, thus reducing the number of available CCN, and the washout of CCN by raindrops. Although in the SO these two processes seem to co-vary (the density of liquid water droplets in the atmosphere displays the same seasonality as the rainfall amount estimates; results not shown), in the present study we focus on the second factor only (below-cloud washout). *Nguyen et al.* [1992] found covariation between wet deposition rates of MSA and nss-SO_4 at Amsterdam Island (38°S, 77° E), a place not far from the northern edge of our study region and characterized by a similar DMS seasonality [*Putaud et al.*, 1992]. Therefore, in the case of using MSA as a proxy for atmospheric DMS, there is no need to introduce rainfall as an extra process because rain effects are already taken into account by the variables (MSA and CCN) themselves. Rather, when using a proxy for atmospheric DMS that does not undergo rain scavenging, like CHL or even DMSw, it is necessary to introduce the rain effects on CCN in the regression model if we seek to explain the CCN seasonality. We would like also to note that not only does the rainfall influence CCN concentration, but it is also influenced by the number of CCN available during cloud formation [*Albrecht*, 1989]. In the presence of high numbers of CCN, owing to the competition for water, the cloud droplets do not grow to larger sizes. Small cloud droplet sizes prevent rainfall and increase cloud lifetime [*Rosenfeld*, 2000; *Matsui et al.*, 2004; *Givati and Rosenfeld*, 2004].

3.2. Statistical Analyses

[20] The monthly average time series for CHL, OH, CCN, RAIN and WIND are used to obtain statistical relationships between variables. First, for each independent variable (CHL, CHL*OH, RAIN and WIND), a simple linear regression against the dependent variable (CCN) is applied. Then a multilinear regression model that relates CCN to CHL*OH and RAIN is developed. The r^2 determination coefficient is used as a measure of the degree of adjustment of the statistical models. The first equation of the multilinear model is based on the assumption that CHL is a proxy for DMS emissions and that DMSa is oxidized to CCN by the OH radical. Assuming that this effect is homogeneously distributed over the entire SO we have

$$\mathrm{CCN} = b * (\mathrm{CHL} * \mathrm{OH}). \tag{1}$$

[21] Then rainfall acts as a sink for CCN, but its effect is not distributed homogeneously: Local rains affect only local CCN concentrations. We thus can consider that, in a given month, only a fraction (S_{rain}) of the total area (S_{tot}) is under the RAIN scavenging effect, with the rest of the area being free of rainfall (S_{free}). We also assume that CCN form a "nonporous layer"; that is, if rainfall occurs, all CCN within the rainy region disappear. This implies that in the S_{rain} area no CCN are present and the satellite is able to see only the CCN in the S_{free} area ($\mathrm{CCN_{sat}}$). The second equation is therefore

$$\mathrm{CCN_{sat}} = \frac{S_{\mathrm{free}}}{S_{\mathrm{free}}} + S_{\mathrm{rain}} * \mathrm{CCN} = \frac{S_{\mathrm{free}}}{S_{\mathrm{tot}}} * \mathrm{CCN}, \tag{2}$$

which in combination with equation (1) becomes

$$\mathrm{CCN_{sat}} = \frac{S_{\mathrm{free}}}{S_{\mathrm{tot}}} * b * (\mathrm{CHL} * \mathrm{OH}). \tag{3}$$

[22] The area fraction free of the rain scavenging effect $\left(\frac{S_{\mathrm{free}}}{S_{\mathrm{tot}}}\right)$ is assumed to be a function of RAIN values: higher rainfall amount implies larger S_{rain} areas. We call this area fraction K(rain). There exists a $\mathrm{RAIN_{max}}$ for when the whole area (S_{tot}) is experiencing rain scavenging (i.e., $S_{\mathrm{free}} = 0$; $K(\mathrm{rain}) = 0$). K(rain) varies between 0 and 1 and can be expressed as a function of the rainfall amount as follows:

$$K(\mathrm{rain}) = \gamma * (\mathrm{RAIN_{max}} - \mathrm{RAIN}_i), \tag{4}$$

where $RAIN_i$ is the rainfall amount and γ is a constant. Then we can rewrite equation (3) as

$$\begin{aligned} CCN_{sat} &= K(\text{rain}) * b * (CHL * OH) \\ &= \gamma * (RAIN_{max} - RAIN_i) * b * (CHL * OH) \\ &= (\gamma * b * RAIN_{max} - \gamma * b * RAIN_i) \times (CHL * OH). \end{aligned} \quad (5)$$

Regrouping constant terms

$$b1 = \gamma * b * RAIN_{max} \quad (6)$$

$$b2 = \gamma * b, \quad (7)$$

we obtain:

$$\begin{aligned} CCN_{sat} &= (b1 - b2 * RAIN_i) * (CHL * OH) \\ &= b1 * (CHL * OH) - b2 * RAIN_i * (CHL * OH). \end{aligned} \quad (8)$$

[23] Not all CCN_{sat} must be related to CHL*OH (i.e., produced exclusively from DMS oxidation). Several authors have found a background level of CCN even when atmospheric MSA (an exclusive product of DMS oxidation) is almost 0, suggesting sources for CCN other than DMS, possibly SS [*Ayers and Gras*, 1991; *Andreae et al.*, 1999]. To account for this background level, we need to add an intercept parameter to the above model, which leads to the final equation,

$$CCN_{sat} = a + b1 * (CHL * OH) - b2 * RAIN_i * (CHL * OH). \quad (9)$$

[24] Parameters a, $b1$ and $b2$ are obtained by a mean square fitting procedure. Conceptually, we can see the second and third terms on the right side of equation (9) as "source" and "sink" terms for CCN, respectively. The former represents the atmospheric oxidative interaction between DMS and OH radical to produce CCN; the second represents the interaction between the potential stock of CCN from DMS oxidation (using CHL*OH as a proxy) and RAIN. The source term is similar to the growth term in ecological models, where a biomass increase is the result of the interaction between the actual biomass stock and nutrient concentration, times a specific growth rate; in the same way, the loss is similar to the predation term, where prey loss is represented by the product of prey biomass and the predation rate.

[25] This kind of model is called an "effective" model, as it is based on average data. The sum of complex nonlinear processes (such as the production, emission and oxidation of biogenic DMS, or the interaction of rainfall and aerosols) is taken as a whole where individual processes are masked and the average behavior is emphasized. Our effective model is then a first order description of the average behavior of the processes; a more complete characterization of the dynamics of the system should be obtained through the use of time dependent differential equations.

4. Results and Discussion

4.1. Linear Regressions

[26] The 2002–2004 time series of CHL, CHL*OH, RAIN and WIND plotted against CCN, as well as their corresponding regression analyses, are shown in Figure 2. CHL and CCN display a strong seasonal coupling (Figure 2a), although in fall and early winter, CHL decrease rates (slopes of the time series curves) are less pronounced than those of CCN. The Spearman correlation coefficient obtained between both variables is high ($\rho = 0.88$, $p\text{-}val \ll 0.001$) and equal to that obtained by *Gabric et al.* [2002] between climatological CHL and AOD (1997–2000) for a region of the SO south of Australia (from 40°S to 53°S and from 126°E to 148°E). The regression analysis also give a similar determination coefficient ($r^2 = 0.82$) to that obtained by *Ayers et al.* [1997] between climatological monthly mean atmospheric DMS and CCN ($r^2 = 0.84$).

[27] The linear regression gives a negative intercept value (-19.52×10^6 partic cm^{-2}; see Figure 2b). This fact is not in agreement with the observations at Cape Grim, where a background level not related to DMS production but most probably to SS was found at about 30–40 CCN cm^{-3} [*Ayers and Gras*, 1991; *Ayers et al.*, 1997; *Andreae et al.*, 1999]. Also, the slope of the CCN versus CHL regression analysis using the normalized data (values divided by its annual mean) is 1.87 (see the equation in brackets in Figure 2b), i.e., more than 3 times higher than the normalized slope obtained by *Ayers et al.* [1997] for CCN versus DMSa (0.52). A reason for this discrepancy is that CHL exhibits lower seasonal amplitude than DMSw and DMSa. A second reason would be the higher seasonal amplitude of our derived CCN compared to those measured at Cape Grim. The summer maximum to winter minimum ratio for CHL is 1.75. On the basis of the *Kettle and Andreae* [2000] DMSw database, the summer maximum to winter minimum ratio for DMSw over the whole SO is about 5, similar to that of DMSa at Cape Grim [*Ayers et al.*, 1995] and 3 times that of CHL. This reflects the differential behavior of CHL and DMS over the annual cycle: they both peak in summer but there is a higher net production of DMS per unit of CHL with respect to wintertime, probably because of the concurrence of phytoplankton succession to higher DMSP producers and plankton physiological stress due to shallow mixing, iron deficiency and high UV exposure [*Simó and Pedrós-Alió*, 1999; *Simó and Dachs*, 2002; *Sunda et al.*, 2002].

[28] The MSA seasonal amplitude is even higher than that of the DMSa (the MSA summer maximum to winter minimum ratio is about 10 [*Andreae et al.*, 1999]). This can be regarded as an indication that some key player(s) is (are) not represented in this correlation analysis. Most likely candidates are the main DMSa oxidant, the OH radical, which is depressed in winter [*Spivakovsky et al.*, 2000], and the main MSA loss factor, rainfall scavenging, which is enhanced in winter. Since both MSA and CCN production from DMS oxidation depend on OH concentration, the correct regression analysis should relate CCN to DMS*OH. This would increase the seasonal amplitude of the independent variable (DMS*OH) and then reduce even more the (normalized) slope. In this regard, the inclusion of the OH radical in our analysis results in a significantly better agreement between CCN and CHL*OH ($\rho = 0.94$, $p\text{-}val \ll 0.001$; see Figure 2c). At the same time we obtain a positive intercept value (3.42×10^6 partic cm^{-2}) and a

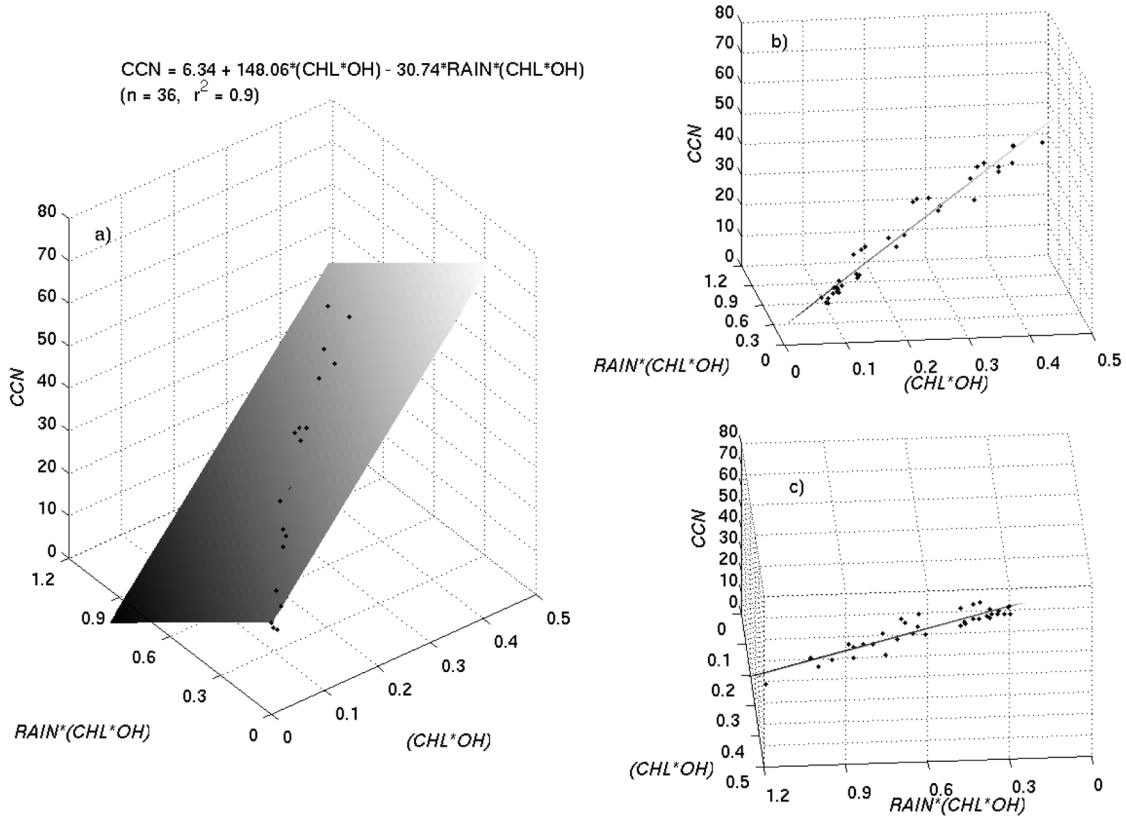

Figure 3. (a) Regression plane obtained for the multilinear regression model that describes CCN column-integrated concentrations (units of 10^6 partic cm^{-2}) as a function of atmospheric DMS oxidation (using ''chlorophyll*hidroxyl radical'' as a proxy) and rainfall washout, for 36 months between January 2002 and December 2004. (b, c) Two different points of view of the regression plane.

(normalized) slope of 0.85 (Figure 2d). We can appreciate how the time series of CHL, CHL*OH and CCN agree in the interannual variability of their annual amplitudes, which increased slightly from January 2002 to December 2004 (see Figures 2a and 2c; CCN retrievals for January 2004 need to be taken with some caution because January 2004 was undersampled).

[29] The monthly mean rainfall amount estimates used in the present study display the same seasonal pattern as the measured rainfall amounts at Cape Grim, with highest values during winter months (wet season) and minima in summer (dry season) [*Ayers and Ivey*, 1990]. The time series of CCN and RAIN show a clear anti-phase trend ($\rho = -0.89$, $p - val \ll 0.001$; see Figure 2e) that is also appreciated in the regression analysis (Figure 2f). However, RAIN displays also lower seasonal amplitude (winter maximum to summer minimum ratio of 1.3) than CCN (ratio of 4; see Figure 2f). Thus RAIN alone cannot be responsible for the CCN seasonality. It is probably the combination of the influences of CHL*OH and RAIN what dictates CCN seasonal evolution.

4.2. Multilinear Regression

[30] While simple linear regression shows a strong coupling between CHL*OH and CCN as well as RAIN and CCN, we also made use of a more advanced multilinear regression model to describe CCN as a function of CHL, OH and RAIN. Multilinear regression allows the reconciliation of the opposite signs of the CHL*OH–CCN relationship (positive) and RAIN–CCN (negative). The model introduces RAIN as a loss process that interacts with the potential production of CCN from CHL through DMS oxidation by OH (see section 3).

[31] The regression plane obtained with the multilinear regression model is plotted in Figure 3a along with the regression equation. Figures 3b and 3c display the distances of the data points to the plane for the ''(CHL*CHL)'' and ''RAIN*(CHL*OH)'' variables, respectively. This analysis shows how CCN rise as CHL*OH increases, and decrease as RAIN goes up (Figures 3a, 3b, and 3c). The determination coefficient is very high ($r^2 = r^2_{adj} = 0.9$; where r^2_{adj} refers to the ''adjusted determination coefficient'' which imposes a penalty for each additional independent variable added to explain the dependent variable CCN [*Ohtani*, 2000]). Thus 90% of the variance in CCN numbers is explained with this multilinear regression model.

[32] Looking at model parameters (see equation in Figure 3a) we can obtain some additional information. The intercept value is 6.34×10^6 partic cm^{-2}, i.e., twice that obtained with the linear model CCN versus CHL*OH.

As expected, both slopes ($b1$ and $b2$) are positive (148.06 and 30.74). This is an a posteriori validation of the model: the conceptual model is not in contradiction with the data. This could seem obvious, but the way we have introduced the effect of rainfall did not necessarily have to be correct and in agreement with the observations. The fact that $b1$ is greater than $b2$ implies that the rainfall amounts present in the SO are well below the theoretical maximum rainfall amount ($RAIN_{max}$) for which all CCN should be cleared out everywhere ($S_{free} = 0$, see section 3). We can easily check this by dividing $b1$ by $b2$, as this fraction will give us the $RAIN_{max}$ (see equations (6) and (7)). The $RAIN_{max}$ obtained is 4.82 mm d^{-1}, a value never achieved within the rainfall amount time series (Figure 2f). In nature, however, the $RAIN_{max}$ that corresponds to a satellite retrieval of zero CCN would be much higher or even infinite. We are able to obtain a $RAIN_{max}$ because we have assumed a linear behavior for K(rain) (see equation (4) in section 3.2) whereas it is probably asymptotic. Nonetheless, within the range of rainfall amounts we are dealing with, such a linear approximation seems to be valid. The relative weights of the production variable "(CHL*OH)" and the sink variable "RAIN*(CHL*OH)" in determining the variability of CCN numbers can be obtained from the standardized slope values of the production and sink terms ($b1s = 1.64$ and $b2s = 0.71$, respectively). The fact that $b1s$ is more than twice $b2s$ indicates that the production is more important than the loss to explain the seasonal CCN pattern.

4.3. Lagged Correlations

[33] Correlations lagging by half a month the atmospheric variables (see section 3) result in a slightly reduction of the level of association between the CHL*OH, RAIN and CCN. The determination coefficient of the linear model CCN versus CHL*OH is now $r^2 = 0.83$ and the determination coefficient obtained with the multilinear model becomes $r^2 = 0.86$. This may indicate that the processes of DMS production, emission and oxidation to CCN are very rapid in the SO, at least during the productive season. However, we have applied a t-test to the correlation coefficients of the linear model obtained with and without the lag and the differences are not statistically significant ($p - val \ll 0.001$).

4.4. Potential Nonbiogenic Sources of CCN

[34] As pointed out by *Gabric et al.* [2002], a major problem associated with monthly series analyses is the possibility of illusory correlations due to an independent seasonal variation of the studied variables. In order to assess whether this can lead to misinterpretation of our results, we need to look at all the factors that could play a controlling role in CHL, OH and CCN seasonality. As we have already noted, CHL seasonality in the SO is mainly governed by light. Solar radiation controls CHL evolution both directly and indirectly. The direct control is due to the higher and longer exposure to photosynthetic active radiation (PAR) during summer. The indirect effect is through the reduction of the MLD: heating of the surface ocean provokes a shoaling of the pycnocline at the same time that PAR is higher, which results in maximum CHL concentrations during summer. In this period only iron seems to be a limiting factor. OH is also driven by solar radiation, in this case by the UV radiation. Regarding the seasonality of aerosols (CCN among them), several are the potential controlling factors: (1) DMS oxidation; (2) SS concentrations; (3) input of continental aerosols (natural or anthropogenic), and (4) rainfall.

[35] The day time oxidation of DMS to give nss-SO_4 aerosols is mediated by OH radicals. As previously mentioned, OH seasonality is coincident with DMS seasonality in the SO. Therefore, summer months would be characterized by both higher DMS emission and better efficiency in the oxidation of DMS into CCN components. In this regard, the mechanistic link proposed between DMS oxidation and nss-SO_4 aerosols has proved to be robust in the SO [*Andreae et al.*, 1999; *Jourdain and Legrand*, 2001]. A good example is the work of *Ayers et al.* [1991] with a 17-month data series, where a strong association between DMS, MSA and nss-SO_4 in both signal amplitude and interannual timing of the peaks can be appreciated. However, it is important to note that although good seasonal associations have also been found between DMS oxidation products and CCN in the SO [*Ayers and Gras*, 1991; *Ayers et al.*, 1995, 1997; *Andreae et al.*, 1999], a mechanistic link has not been completely confirmed because the relative contribution of nss-SO_4 to the composition of CCN is still object of discussion [*O'Dowd et al.*, 1997; *Murphy et al.*, 1998]. Variable amounts of nss-SO_4 can be internally mixed with SS [*O'Dowd et al.*, 1997, 1999; *Alexander et al.*, 2005] bringing up more efficient CCN [*Murphy et al.*, 1998] and small SS can compete with nss-SO_4 for the accumulation mode [*O'Dowd et al.*, 1997; *Ghan et al.*, 1998].

[36] SS aerosol mass concentrations are high in the SO [*Murphy et al.*, 1998; *Quinn et al.*, 1998]. However, their contribution to the numbers of small aerosols is low. After a cruise across the Pacific Ocean that also traversed the SO, *McInnes et al.* [1997] reported that SS aerosols between 0.1 and 1 μm represented only 4–7% of the total number of particles in this range, but 86–100% of supermicron particles with a mean diameter of 1.5 μm. SS aerosol is formed by mechanical interaction of wind with the sea surface, particularly through bursting of air bubbles during whitecap formation and wave breaking. Thus, SS production can be qualitatively estimated from wind speed, even though the correlation between SS and wind speed in the SO is not as high as should be expected [*Andreae et al.*, 1999]. As illustrated by Figure 2h, WIND shows little seasonal variability (values within the narrow range of 9.5–11.5 m s^{-1}), in agreement with what has been reported by *Gille* [2005]. This contrasts with the high seasonal amplitude of CCN. Moreover, WIND seasonality is characterized by a slight increase in winter [*Ayers et al.*, 1999; *Andreae et al.*, 1999] when CCN are at their annual minimum (Figure 2g). All these facts are consistent with the low seasonal variability of SS reported for the SO with a slight maximum in winter [*Wangenbach et al.*, 1998; *Ayers et al.*, 1999; *Andreae et al.*, 1999; *Gong et al.*, 1997, 2002; *Grini et al.*, 2002; *Easter et al.*, 2004]. Our results suggest that SS aerosol production is not responsible for the observed CCN seasonality, in agreement with the observations made at Cape Grim by *Andreae*

et al. [1999], who found that CCN and SS were not correlated. It could be argued that, if SS aerosol production in the SO is rather constant throughout the year, we might expect SS aerosols follow the seasonality of the rainfall amount and be depressed during the wet season, just like CCN. The reason for this not happening is that SS aerosol production by wind friction is a very rapid process [*Andreas*, 1998; *Smirnov et al.*, 2003], and the cold fronts responsible for increases in rainfall are generally associated with local wind storms that cause higher SS production. Then the replacement of the SS washed out by rain would occur almost instantaneously, and the rain effect would not become apparent on a monthly basis. Such a hypothesis is in agreement with the modeling work of *Grini et al.* [2002], who showed higher wintertime SS wet deposition co-occurring with higher SS production, with a net result of slightly higher SS concentrations.

[37] Another potential source of CCN is continental aerosols (the fine mode of dust, organic carbon in smoke and anthropogenic nss-SO_4). The SO is scarcely impacted by continental aerosols [*Husar et al.*, 1997; *Kaufman et al.*, 2002; *Higurashi et al.*, 2000]. Anthropogenic sources of nss-SO_4 are mainly located in the Northern Hemisphere [*Bates et al.*, 1992], being the SO relatively free of such emissions [*Gabric et al.*, 2001]. Even though a fraction of oceanic aerosols during ACE-1 contained soot [*Buseck and Pósfai*, 1999], very little soot was found by *McInnes et al.* [1997] during a ship transect from 67°S to 48°N over the Pacific Ocean, where SO_4 was the dominant aerosol component. Dust fluxes to the SO are also amongst the weakest of the world's oceans [*Jickells et al.*, 2005]. *Gao et al.* [2001] pointed out that the SO has extremely low atmospheric concentrations of iron, reflecting little influence by dust transport throughout the year. Nonetheless, dust storm activity in south west Australia is higher in summer [*McTainsh et al.*, 1998; *Gabric et al.*, 2002]. In this period, the monthly average dust storm frequency is in the range of 0.06–0.12, i.e., 2 to 4 dust storms per month. Such a low activity would be smoothed out in the monthly means of satellite CCN retrieval. *Herman et al.* [1997] analyzed satellite data from the Total Ozone Mapping Spectrometer (TOMS, NASA) and did not found detectable amounts of UV absorbing aerosols (e.g., dust, soot, smoke) over the SO in any month of the year. With respect to black carbon aerosols (soot and smoke), the closest sources (South America and South Africa) have their higher emissions roughly from June to September (austral winter) [*Herman et al.*, 1997; *Kaufman et al.*, 2002]. Similarly, carbon monoxide seasonality in the SO peaks in September–October and is at its minimum during January–February [*Spivakovsky et al.*, 2000] coinciding with a summer minimum in biomass burning activity [*Duncan et al.*, 2003]. Thus the potential contribution of organic carbon to the CCN burden, if any, should occur only in late winter–early spring.

4.5. Fine Mode Aerosols

[38] Further indication of the seasonal decoupling between CCN and SS particles or dust, and support for a biogenic origin of the former, can be obtained from the study of the MODIS primary parameter ETA (the fraction of AOD accounted for by the accumulation mode, see section 3.1). As previously stated, SS and dust are mainly composed of coarse particles while nss-SO_4 belongs to the accumulation mode. Although MSA can be present in the accumulation and coarse modes (*Bates et al.* [1998] reported that during ACE 1, MSA mass was almost evenly distributed in both modes), its mass contribution to the aerosol burden is much lower than nss-SO_4 [*Bates et al.*, 1998; *Jourdain and Legrand*, 2001]. If DMS oxidation were a major source of aerosols during summer months, the ETA parameter would be highly influenced by nss-SO_4 seasonality and then it should be higher in summer. On the contrary, a summer increase of SS or dust would be reflected as a decrease of the ETA parameter. Figure 4 shows the time evolution of ETA. It displays a marked seasonality where the contribution of the small mode particles to the total AOD increases by a factor of 3.5 in summer with respect to winter (from 13% to 45%). Therefore, although the absolute contribution of the small aerosols to the total aerosol burden is relatively low (an annual average of 30%) owing to the presence of high (and almost constant) amounts of SS aerosols [*Andreae et al.*, 1999], the seasonality of the small mode aerosols is mostly driven by the biological oceanic source.

[39] The aforementioned facts can be used to estimate the biogenic contribution to CCN numbers. If the total aerosol burden in the SO is assumed to be composed mainly of nss-SO_4, SS and (to a lesser extent) MSA [*Quinn et al.*, 1998], CCN would be contributed mainly by nss-SO_4, SS_{small} and MSA_{small}. Then CCN can be expressed as

$$CCN = CCN_{bio} + SS_{small}, \tag{10}$$

where CCN_{bio} = nss-SO_4 + MSA_{small}. Assuming that the intercept value of the multilinear model corresponds to a background (and almost constant) level of SS [*Andreae et al.*, 1999] (SS_{small}, since CCN is contributed only by particles between 0.1 and 1 μm), we obtain CCN_{bio} = CCN − SS_{small}. CCN_{bio} varies from about 3×10^6 partic cm^{-2} in winter to 30×10^6 partic cm^{-2} in summer. That is, a seasonal amplitude of a factor of 10, which is exactly the seasonal amplitude of MSA at Cape Grim [*Andreae et al.*, 1999]. We can thus define the contribution of biogenic CCN to the total CCN as BETA = CCN_{bio}/CCN. The seasonal evolution of the estimated BETA is plotted in Figure 4. We can appreciate that the biogenic contribution to the CCN has an average value of 35% in winter months and 80% in summer (the remaining CCN being contributed by SS_{small}). Thus CCN seasonality in the SO seems to be highly influenced by CCN_{bio} seasonality.

5. Conclusions

[40] We have performed statistical linear regression analyses with the aim at looking for functional relationships between monthly means of satellite-derived CCN, surface ocean CHL, OH radical and RAIN for the entire SO. Triannual time series (from January 2002 to December 2004) of these variables have been used to explain the

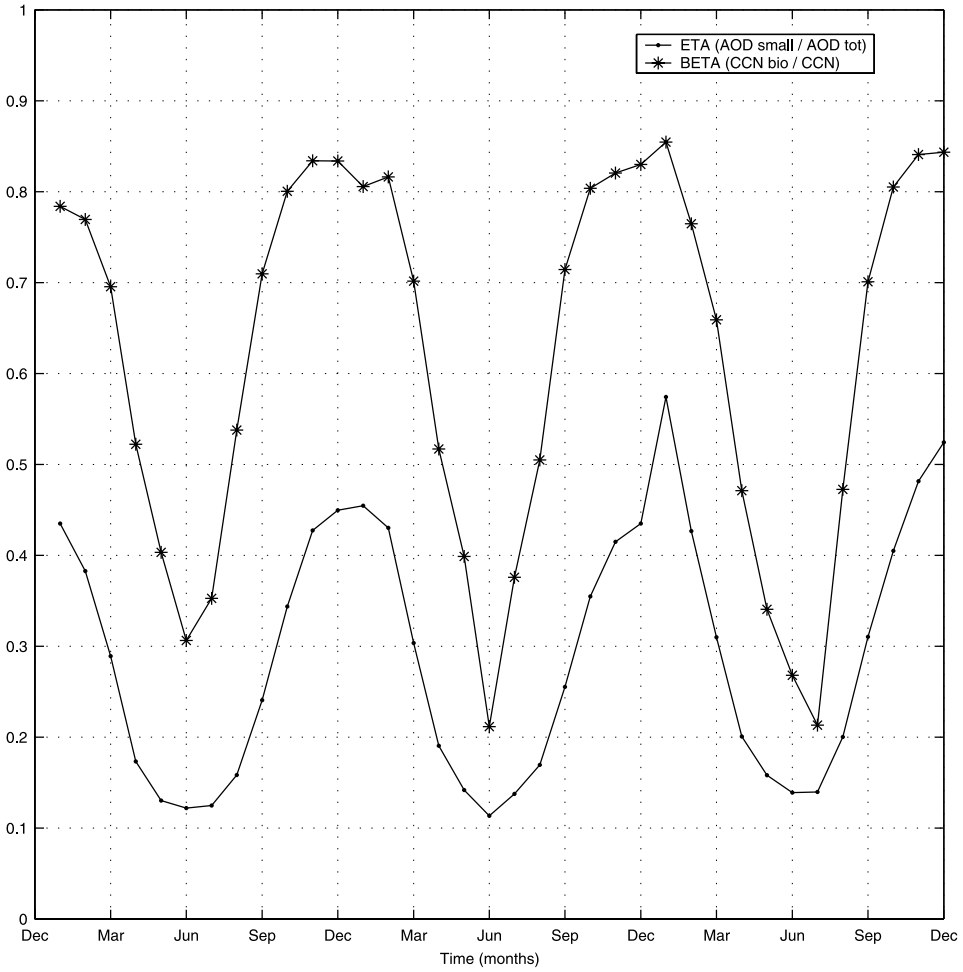

Figure 4. Seasonal evolution (years 2002 to 2004) of the contribution of small mode particles to the Aerosol Optical Depth (ETA parameter = AOD_{small}/AOD_{total}) as provided by MODIS, and seasonal evolution (years 2002 to 2004) of the estimated contribution of biogenic CCN to the total CCN burden (BETA = CCN_{bio}/CCN).

seasonality of CCN in this pristine region. A multilinear regression model has revealed that the seasonal and interannual variability of potential CCN is highly explained by the variability of CHL (as a proxy for the emission of the planktonic aerosol precursor DMS), OH (as the main oxidizer of atmospheric DMS) and rainfall. This is in agreement with local experimental studies where relationships between biogenic DMS and its aerosol products have been observed, as well as with the central role of rainfall in removing atmospheric submicron aerosols. Although statistical analyses could never serve as a proof for causal relationships between variables, and other factors (like those related to atmospheric dynamics and in-cloud aerosol processing) that can influence the CCN seasonal variability cannot be ruled out, their full exploration is beyond the scope of the present study. At the present stage, our results suggest that the seasonal correlations found between CHL*OH, RAIN and CCN are not independently driven by third variables but seem to be linked through causal relationships. The main arguments for such a conclusion are: (1) the strong association observed between CHL*OH and CCN, with some interannual association also captured; (2) the anti-phase association between CCN and WIND; (3) the low detectable influence of continentally derived aerosols on CCN numbers over the SO; and (4) the seasonality of the ETA parameter, which shows a 3.5 times increase from winter to summer despite the high (and almost constant) contribution of SS to the total AOD. Therefore the high determination coefficients and significance obtained with the regression models applied strongly support the hypothesis that oceanic microbiota affect CCN concentrations through the production, emission and atmospheric oxidation of DMS at large spatial scales. Given that CCN concentrations are modulated by oceanic DMS, it is very probable that cloud formation and their properties are affected too, with important implications for climate as proposed by *Charlson et al.* [1987] 18 years ago. We suggest that this kind of statistical approach, based mainly on satellite measurements and model data, should be applied to other oceanic regions and expanded to the global

scale. Along with continued fieldwork, it should be very useful in future research addressing the validity of the CLAW hypothesis and its implications in Earth System functioning and Global Change.

[41] **Acknowledgments.** This work is part of the AMIGOS project, funded by the Spanish Ministerio de Ciencia y Tecnología. Our special thanks go to A. Turiel for his helpful ideas regarding the multiple regression model and to E. Pallás-Sanz for many fruitful discussions, and to E. Jurado and J. Dachs for assistance with the handling and processing of satellite data. The authors would also like to thank the SeaWiFS, MODIS-Atmosphere, and NCEP/NCAR Reanalysis Projects for the production and free distribution of some of the data used in the present work, and two anonymous reviewers for their relevant comments and suggestions that have improved significantly the final version of the manuscript.

References

Albrecht, B. A. (1989), Aerosols, cloud microphysics, and fractional cloudiness, *Science*, *245*, 1227–1230.

Alexander, B., R. J. Park, D. J. Jacob, Q. B. Li, R. M. Yantosca, J. Savarino, C. C. W. Lee, and M. H. Thiemens (2005), Sulfate formation in sea-salt aerosols: Constraints from oxygen isotopes, *J. Geophys. Res.*, *110*, D10307, doi:10.1029/2004JD005659.

Andreae, M. O., and P. J. Crutzen (1997), Atmospheric aerosols: Biogeochemical sources and role in the atmospheric chemistry, *Science*, *276*, 1052–1058.

Andreae, M. O., W. Elbert, Y. Cai, and T. W. Andreae (1999), Non-sea-salt sulfate, methanesulfonate, and nitrate aerosol concentrations and size distributions at Cape Grim, Tasmania, *J. Geophys. Res.*, *104*(D1), 21,695–21,706.

Andreas, E. L. (1998), A new sea spray generation function for wind speeds up to 32 m/s, *J. Phys. Oceanogr.*, *28*(11), 2175–2184.

Ayers, G. P., and R. W. Gillett (2000), DMS and its oxidation products in the remote marine atmosphere: Implications for climate and atmospheric chemistry, *J. Sea Res.*, *43*, 275–286.

Ayers, G. P., and J. L. Gras (1991), Seasonal relationship between cloud condensation nuclei and aerosol methanesulphonate in marine air, *Nature*, *353*, 834–835.

Ayers, G. P., and J. P. Ivey (1990), Methanesulfonate in rainwater at Cape Grim, Tasmania, *Tellus, Ser. B*, *42*, 217–222.

Ayers, G. P., J. P. Ivey, and R. W. Gillett (1991), Coherence between seasonal cycles of dimethyl sulphide, methanesulphonate and sulphate in marine air, *Nature*, *349*, 404–406.

Ayers, G. P., J. P. Ivey, and B. W. Forgan (1995), Dimethylsulfide in marine air at Cape Grim, 41°S, *J. Geophys. Res.*, *100*(D10), 21,013–21,021.

Ayers, G. P., J. M. Cainey, R. W. Gillett, and J. P. Ivey (1997), Atmospheric sulphur and cloud condensation nuclei air in marine air in the Southern Hemisphere, *Philos. Trans. R. Soc. London, Ser. B*, *352*, 203–211.

Ayers, G. P., R. W. Gillett, J. M. Cainey, and A. L. Dick (1999), Chloride and bromide loss from sea-salt particle in Southern Ocean air, *J. Atmos. Chem.*, *33*, 299–319.

Bates, T. S., B. K. Lamb, A. Guenther, J. Dignon, and R. E. Stoiber (1992), Sulfur emissions to the atmosphere from natural sources, *J. Atmos. Chem.*, *14*, 315–337.

Bates, T. S., V. N. Kapustin, P. K. Quinn, D. S. Covert, D. J. Coffman, C. Mari, P. A. Durkee, W. J. De Bruyn, and E. S. Saltzman (1998), Processes controlling the distribution of aerosol particles in the lower marine boundary layer during the First Aerosol Characterization Experiment (ACE 1), *J. Geophys. Res.*, *103*(D13), 16,369–16,383.

Benkovitz, C. M., M. T. Scholtz, J. Pacyna, L. Tarrasón, J. Dignon, E. C. Voldner, P. A. Spiro, J. A. Logan, and T. E. Graedel (1996), Global gridded inventories of anthropogenic emissions of sulfur and nitrogen, *J. Geophys. Res.*, *101*(D22), 29,239–29,253.

Boyd, P. W. (2002), Environmental factors controlling phytoplankton processes in the Southern Ocean, *J. Phycol.*, *38*, 844–861.

Boyd, P. W., et al. (2000), Amesoscale phytoplankton bloom in the polar Southern Ocean stimulated by iron fertilization, *Nature*, *407*, 695–702.

Brechtel, F. J., S. M. Kreidenweis, and H. B. Swan (1998), Air mass characteristics, aerosol particle number concentrations, and number size distributions at Macquarie Island during the First Aerosol Characterization Experiment (ACE 1), *J. Geophys. Res.*, *103*(D13), 16,351–16,367.

Buseck, P. R., and M. Pósfai (1999), Aireborne minerals and related aerosol particles: Effects on climate and the environment, *Proc. Natl. Acad. Sci. U. S. A.*, *96*, 3372–3379.

Chapman, E. G., W. J. Shaw, R. C. Easter, X. Bian, and S. J. Ghan (2002), Influence of wind speed averaging on estimates of dimethylsulfide emission fluxes, *J. Geophys. Res.*, *107*(D23), 4672, doi:10.1029/2001JD001564.

Charlson, R. J., J. E. Lovelock, M. O. Andreae, and S. G. Warren (1987), Oceanic phytoplankton, atmospheric sulfur, cloud albedo and climate, *Nature*, *326*, 655–661.

Cox, R. A. (1997), Atmospheric sulphur and climate: What have we learned?, *Philos. Trans. R. Soc. London, Ser. B*, *352*, 251–254.

Curran, M. A. J., and G. B. Jones (2000), Dimethylsulfide in the Southern Ocean: Seasonality and flux, *J. Geophys. Res.*, *105*(D16), 20,451–20,459.

Dacey, J. W. H., F. A. Howse, A. F. Michaels, and S. G. Wakeham (1998), Temporal variability of dimethylsulfide and dimethylsulfoniopropionate in the Sargasso Sea, *Deep Sea Res., Part I*, *45*, 2085–2104.

de Boyer-Montégut, C., G. Madec, A. S. Fischer, A. Lazar, and D. Iudicone (2004), Mixed layer depth over the global ocean: An examination of profile data and a profile-based climatology, *J. Geophys. Res.*, *109*, C12003, doi:10.1029/2004JC002378.

Duncan, N. B., R. V. Martin, A. C. Staudt, R. Yevich, and J. A. Logan (2003), Interannual and seasonal variability of biomass burning emissions constrained by satellite observations, *J. Geophys. Res.*, *108*(D2), 4100, doi:10.1029/2002JD002378.

Easter, C. R., S. J. Ghan, Y. Zhang, R. D. Saylor, E. G. Chapman, N. S. Laulainen, H. Abdul-Razzak, L. R. Leung, X. Bian, and A. Zaveri (2004), MIRAGE: Model description and evaluation of aerosols and trace gases, *J. Geophys. Res.*, *109*, D20210, doi:10.1029/2004JD004571.

Fiore, A. M., D. J. Jacob, H. Liu, R. M. Yantosca, T. D. Fairlie, and Q. B. Li (2003), Variability in surface ozone background over the United States: Implications for air quality policy, *J. Geophys. Res.*, *108*(D24), 4787, doi:10.1029/2003JD003855.

Fitzgerald, J. W. (1991), Marine aerosols: A review, *Atmos. Environ., Part A*, *25*(3–4), 533–545.

Gabric, A., G. Ayers, C. N. Murray, and J. Parslow (1996), Use of remote sensing and mathematical modelling to predict the flux of dimethylsulphide to the atmosphere in the Southern Ocean, *Adv. Space Res.*, *18*(7), 117–128.

Gabric, A. J., P. H. Whetton, and R. Cropp (2001), Dimethylsulphide production in the subantarctic Southern Ocean under enhanced greenhouse conditions, *Tellus, Ser. B*, *53*, 273–287.

Gabric, A. J., R. Cropp, G. P. Ayers, G. McTainsh, and R. Braddock (2002), Coupling between cycles of phytoplankton biomass and aerosol optical depth as derived from SeaWiFS time series in the subantartic Southern Ocean, *Geophys. Res. Lett.*, *29*(7), 1112, doi:10.1029/2001GL013545.

Gao, Y., Y. J. Kaufman, D. Tanré, D. Kolber, and P. G. Falkowski (2001), Seasonal distributions of aeolian iron fluxes to the Global Ocean, *Geophys. Res. Lett.*, *28*(1), 29–32.

Gassó, S., and D. A. Hegg (2003), On the retrieval of columnar aerosol mass and CCN concentration by MODIS, *J. Geophys. Res.*, *108*(D1), 4010, doi:10.1029/2002JD002382.

Ghan, S. J., G. Guzman, and H. Abdul-Razzak (1998), Competition between sea salt and sulphate particles as cloud condensation nuclei, *J. Atmos. Sci.*, *55*(22), 3340–3347.

Gille, S. T. (2005), Statistical characterization of zonal and meridional ocean wind stress, *J. Atmos. Oceanic Technol.*, in press.

Givati, A., and D. Rosenfeld (2004), Quantifying precipitation suppression due to air pollution, *J. Appl. Meteorol.*, *43*, 1038–1056.

Gong, S. L., L. A. Barrie, J. M. Prospero, D. L. Savoie, G. P. Ayers, J.-P. Blanchet, and L. Spacek (1997), Modeling sea-salt aerosols in the atmosphere: 2. Atmospheric concentrations and fluxes, *J. Geophys. Res.*, *102*(D3), 3819–3830.

Gong, S. L., L. A. Barrie, and M. Lazare (2002), Canadian Aerosol Module (CAM): A size-segregated simulation of atmospheric aerosol processes for climate and air quality models: 2. Global sea-salt aerosol and its budgets, *J. Geophys. Res.*, *107*(D24), 4779, doi:10.1029/2001JD002004.

Grini, A., G. Myhre, J. K. Sundet, and I. S. A. Isaken (2002), Modeling the annual cycle of sea salt in the global 3D Model Oslo CTM2: Concentrations, fluxes, and radiative impact, *J. Clim.*, *15*, 1717–1730.

Herman, J. R., P. K. Bhartia, O. Torres, C. Hsu, C. Seftor, and E. Celarier (1997), Global distributions of UV-absorbing aerosols from Nimbus 7/TOMS data, *J. Geophys. Res.*, *102*(D14), 16,911–16,922.

Higurashi, A., T. Nakajima, B. N. Holben, A. Smirnov, R. Frouin, and B. Chatenet (2000), A study of global aerosol optical climatology with two channel AVHRR remote sensing, *J. Clim.*, *13*, 2011–2027.

Hudson, G. J., X. Yonghong, and S. S. Yum (1998), Vertical distributions of cloud condensation nuclei spectra over the summertime Southern Ocean, *J. Geophys. Res.*, *103*(D13), 16,609–16,624.

Husar, R. B., J. M. Prospero, and L. L. Stowe (1997), Characterization of tropospheric aerosols over the oceans with the NOAA advanced very high resolution radiometer optical thickness operational product, *J. Geophys. Res.*, *102*(D14), 16,889–16,909.

Jickells, T. D., et al. (2005), Global iron connections between desert dust, ocean biogeochemistry, and climate, *Science*, *308*, 67–71.

Jourdain, B., and M. Legrand (2001), Seasonal variations of atmospheric dimethylsulfide, dimethylsulfoxide, sulfur dioxide, methanesulfonate, and non-sea-salt sulfate aerosols at Dumont d'Urville (coastal Antarctica) (December 1998 to July 1999), *J. Geophys. Res.*, *106*(D13), 14,391–14,408.

Kaufman, Y. J., D. Tanre, and O. Boucher (2002), A satellite view of aerosols in the climate system, *Nature*, *419*, 215–223.

Kettle, A. J., and M. O. Andreae (2000), Flux of dimethylsulfide from the oceans: A comparison of updated data set and flux models, *J. Geophys. Res.*, *105*(D22), 26,793–26,808.

Kettle, A. J., et al. (1999), A global database of sea surface dimethylsulfide (DMS) measurements and a simple model to predict sea surface DMS as a function of latitude, longitude and month, *Global Biogeochem. Cycles*, *13*, 399–444.

Kistler, R., et al. (2001), The NCEP-NCAR 50-Year Reanalysis: Monthly means CD-ROM and documentation, *Bull. Am. Meteorol. Soc.*, *82*(2), 247–267.

Liss, P. S., and L. Merlivat (1986), Air-seagas exchange rates: Introduction and synthesis, in *The Role of Sea-Air Exchange in Geochemical Cycling 1986*, edited by P. Buat-Menard, pp. 113–127, Springer, New York.

Mari, C., K. Suhre, T. S. Bates, J. E. Johnson, R. Rosset, A. R. Bandy, F. L. Eisele, R. L. Mauldin III, and D. C. Thornton (1998), Physico-chemical modeling of the First Aerosol Characterization Experiment (ACE 1) Lagrangian B: 2. DMS emission, transport and oxidation at the mesoscale, *J. Geophys. Res.*, *103*(D13), 16,457–16,473.

Matsui, T., H. Masunaga, R. Pielke, and W. Tao (2004), Impact of aerosols and atmospheric thermodynamics on cloud properties within the climate system, *Geophys. Res. Lett.*, *31*(6), L06109, doi:10.1029/2003GL019287.

McInnes, L., D. Covert, and B. Baker (1997), The number of sea-salt, sulfate, and carbonaceous particles in the marine atmosphere: EM measurements consistent with ambient size distribution, *Tellus, Ser. B*, *49*, 300–313.

McTainsh, G. H., A. W. Lynch, and E. K. Tews (1998), Climatic controls upon dust storm occurrence in eastern Australia, *J. Arid Environ.*, *39*, 457–466.

Moore, J. K., and M. R. Abbott (2000), Phytoplankton chlorophyll distributions and primary production in the Southern Ocean, *J. Geophys. Res.*, *105*(C12), 28,709–28,722.

Moore, J. K., M. R. Abbott, and J. G. Richman (1999), Location and dynamics of the Antarctic Polar Front from satellite sea surface temperature data, *J. Geophys. Res.*, *104*(C2), 3059–3073.

Murphy, D. M., J. R. Anderson, P. K. Quinn, L. M. McInnes, F. J. Brechtel, S. M. Kreidenweis, A. M. Middlebrook, M. Pósfai, D. S. Thomson, and P. R. Buseck (1998), Influence of sea-salt on aerosol radiative properties in the Southern Ocean marine boundary layer, *Nature*, *392*, 62–65.

Nguyen, B. C., N. Mihalopoulos, J. P. Putaud, A. Gaudry, and L. Gallet (1992), Covariations in oceanic dimethyl sulfide, its oxidation products and rain acidity at Amsterdam Island in the Southern Indian Ocean, *J. Atmos. Chem.*, *15*, 39–53.

O'Dowd, C. D., J. A. Lowe, M. H. Smith, B. Davison, C. N. Hewitt, and R. M. Harrison (1997), Biogenic sulphur emissions and inferred non-sea-salt-sulphate cloud condensation nuclei in and around Antarctica, *J. Geophys. Res.*, *102*(D11), 12,839–12,854.

O'Dowd, C. D., J. A. Lowe, and M. H. Smith (1999), Coupling sea-salt and sulphate interactions and its impact on cloud droplet concentration predictions, *Geophys. Res. Lett.*, *26*(9), 1311–1314.

Ohtani, K. (2000), Bootstrapping r^2 and adjusted r^2 in regression analysis, *Econ. Modell.*, *17*, 473–483.

Prospero, J. M., D. L. Savoie, E. S. Saltzman, and R. Larsen (1991), Impact of oceanic sources of biogenic sulphur on sulphate aerosol concentrations at Mawson, Antarctica, *Nature*, *350*, 221–223.

Prospero, J. M., P. Ginoux, O. Torres, S. E. Nicholson, and T. E. Gill (2002), Environmental characterization of global sources of atmospheric soil dust identified with the Nimbus 7 Total Ozone Mapping Spectrometer (TOMS) absorbing aerosol product, *Rev. Geophys.*, *40*(1), 1002, doi:10.1029/2000RG000095.

Putaud, J. P., N. Mihalopoulos, B. C. Nguyen, and J. M. Campin (1992), Seasonal variations of atmospheric sulfur dioxide and dimethylsulfide concentrations at Amsterdam Island in the Southern Indian Ocean, *J. Atmos. Chem.*, *15*, 117–131.

Quinn, P. K., D. J. Coffman, V. N. Kapustin, and T. S. Bates (1998), Aerosol optical properties in the marine boundary layer during the First Aerosol Characterization Experiment (ACE 1) and the underlying chemical and physical aerosol properties, *J. Geophys. Res.*, *103*(D13), 16,547–16,563.

Rasmus, K. E., W. Granéli, and S.-Å. Wängberg (2004), Optical studies in the Southern Ocean, *Deep Sea Res., Part II*, *51*, 2583–2597.

Remer, L. A., et al. (2005), The MODIS aerosol algorithm, products and validation, *J. Atmos. Sci.*, *62*, 947–973.

Rosenfeld, D. (2000), Suppression of rain and snow by urban and industrial air pollution, *Science*, *287*, 1793–1796.

Savoie, D. L., and J. M. Prospero (1989), Comparison of oceanic and continental sources of non-sea-salt sulphate over the Pacific Ocean, *Nature*, *339*, 685–687.

Shon, Z.-H., et al. (2001), Evaluation of the DMS flux and its conversion to SO_2 over the Southern Ocean, *Atmos. Environ.*, *35*(1), 159–172.

Simó, R. (2001), Production of atmospheric sulfur by oceanic plankton: Biogeochemical, ecological and evolutionary links, *Trends Ecol. Evol.*, *16*(6), 287–294.

Simó, R., and J. Dachs (2002), Global ocean emission of dimethylsulfide predicted from biogeophysical data, *Global Biogeochem. Cycles*, *16*(4), 1018, doi:10.1029/2001GB001829.

Simó, R., and C. Pedrós-Alió (1999), Role of vertical mixing in controlling the oceanic production of dimethyl sulphide, *Nature*, *402*, 396–399.

Smirnov, A., B. N. Hoben, T. F. Eck, O. Dubovik, and I. Slutsker (2003), Effect of wind speed on columnar aerosol optical properties at Midway Island, *J. Geophys. Res.*, *108*(D24), 4802, doi:10.1029/2003JD003879.

Spivakovsky, C. M., et al. (2000), Three-dimensional climatological distribution of tropospheric OH: Update and evaluation, *J. Geophys. Res.*, *105*(D7), 8931–8980.

Stefels, J. (2000), Physiological aspects of the production and conversion of DMSP in marine algae and higher plants, *J. Sea Res.*, *43*, 183–197.

Sunda, W., D. J. Kleber, R. P. Kiene, and S. Huntsman (2002), An antioxidant function for DMSP and DMS in marine algae, *Nature*, *418*, 317–320.

Tanré, D., L. A. Remer, Y. J. Kaufman, S. Mattoo, P. V. Hobbs, J. M. Livingston, P. B. Russell, and A. Smirnov (1999), Retrieval of aerosol optical thickness and size distribution over ocean from the MODIS airborne simulator during TARFOX, *J. Geophys. Res.*, *104*(D2), 2261–2278.

Toole, D. A., and D. A. Siegel (2004), Light-driven cycling of dimethylsulfide (DMS) in the Sargasso Sea: Closing the loop, *Geophys. Res. Lett.*, *31*, L09308, doi:10.1029/2004GL019581.

Turner, D., and N. J. P. Owens (1995), A biogeochemical study in the Bellingshausen Sea: Overview of the STERNA 1992 expedition, *Deep Sea Res., Part II*, *42*, 907–932.

Wangenbach, D., F. Ducroz, R. Mulvaney, L. Keck, A. Minikin, M. Legrand, J. S. Hall, and E. W. Wolff (1998), Sea-salt aerosol in coastal Antarctic regions, *J. Geophys. Res.*, *103*(D9), 10,961–10,974.

Yang, H., and H. R. Gordon (1997), Remote sensing of ocean color: Assessment of the water-leaving radiance bidirectional effects on the atmospheric diffuse transmittance, *Appl. Opt.*, *36*(30), 7887–7897.

Yuan, X. (2004), High-speed evaluation in the Southern Ocean, *J. Geophys. Res.*, *109*, D13101, doi:10.1029/2003JD004179.

S. Gassó, Goddard Earth Science and Technology Center, University of Maryland Baltimore County, Baltimore, MD 21250, USA.

R. Simó and S. M. Vallina, Institut de Ciències del Mar–Consejo Superior de Investigaciones Científicas (ICM–CSIC), Passeig Marítim de la Barcelona, 37-49, E-08003 Barcelona, Spain. (sergio.vallina@icm.csic.es)